Towards understanding microbial degradation of chloroquine in large saltwater systems

Jinglin Hu, Nancy Hellgeth, Chrissy Cabay, James Clark, Francis J. Oliaro, William Van Bonn, Erica M. Hartmann

PII: S0048-9697(21)05609-6

DOI: https://doi.org/10.1016/j.scitotenv.2021.150532

Reference: STOTEN 150532

To appear in: *Science of the Total Environment*

Received date: 14 June 2021

Revised date: 30 August 2021

Accepted date: 19 September 2021

Please cite this article as: J. Hu, N. Hellgeth, C. Cabay, et al., Towards understanding microbial degradation of chloroquine in large saltwater systems, *Science of the Total Environment* (2018), https://doi.org/10.1016/j.scitotenv.2021.150532

Towards Understanding Microbial Degradation of Chloroquine in Large Saltwater Systems

Jinglin Hu[1], Nancy Hellgeth[1], Chrissy Cabay[2], James Clark[2], Francis J. Oliaro[2] and William Van Bonn[2], Erica M. Hartmann[1*]

[1] Department of Civil and Environmental Engineering, Northwestern University, Evanston, IL, USA

[2] Animal Care and Science Division, John G. Shedd Aquarium, Chicago, IL, USA

*Corresponding author:

Erica M. Hartmann

2145 Sheridan Road

Tech A322

Evanston, IL 60208-3109

847-467-4528

erica.hartmann@northwestern.edu

Abstract

Circulating saltwater aquariums hosting marine animals contain a wide range of microorganisms, which have strong implications on promoting animal health. In this study, we investigated the degradation of chloroquine phosphate, an anti-parasitic bath pharmaceutical used in saltwater quarantine and exhibition systems, and attributed the reduction in drug concentration to microbial degradation of chloroquine associated with pipeline microbial communities. To advance our knowledge on chloroquine degradation in aquatic systems, we conducted microbial and chemical analyses on three tropical saltwater systems. Our findings show that aquarium microbiome composition is shaped by sampling location (i.e., tank water and pipeline; PERMANOVA R^2 = 0.09992, p = 0.0134), chloroquine dosing (PERMANOVA R^2 = 0.05700, p = 0.0030), and whether the aquarium is occupied by marine animals (PERMANOVA R^2 = 0.07019, p = 0.0009). Several microbial taxa belonging to the phyla *Actinobacteria*, *Bacteroidetes*, *Chloroflexi*, and *Proteobacteria*, along with functional genes related to pathways such as phenylethylamine degradation and denitrification, appeared to have differential (relative) abundance between samples where chloroquine degradation was observed and those without degradation (Benjamini-Hochberg adjusted p-value < 0.05). Together, these results provide practical mitigation options to prevent or delay the development of chloroquine-degrading microbial communities in saltwater aquariums. Our results further demonstrate the need to improve our understanding of the interactions between nitrogen availability and microbial activity in saltwater systems.

Keywords

Aquarium microbiome; Chloroquine degradation; Management of circulating aquarium systems; Animal health; Aquarium antiparasitic drugs; Nitrogen cycling

Highlights

- Microbial processes dominate the degradation of chloroquine in saltwater aquariums.
- Pipeline communities represent the main contributors to chloroquine degradation.
- Nitrogen limitation likely affects chloroquine degradation in saltwater aquariums.

1. Introduction

Chloroquine ($C_{18}H_{26}ClN_3$), a 4-aminoquinoline derivative, is an anti-parasitic drug widely used as a bath pharmaceutical for external protozoa infection control in aquariums, ranging from small in-house fish tanks to large public aquariums. At public display aquariums, chloroquine phosphate along with copper sulfate are commonly used in response to white dot diseases caused by *Cryptocaryon irritans* [1], a ciliated protozoan ectoparasite. Such parasitic outbreaks can be harmful or even deadly to a wide range of marine animals, especially those that are under stress from activities such as long-distance transport [2, 3]. To effectively remove *Cryptocaryon irritans*, a bath treatment should last for 14 to 21 days, during which time the chloroquine concentration needs to be maintained above a therapeutic dose determined by professional veterinarians (10 mg/L in this study). In the last four years, multiple exhibitions and quarantine systems treated with chloroquine at Shedd and other aquariums underwent minimal to severe chloroquine degradation and the therapeutic dose could not be maintained for the 14-day prescribed period, even with continuous and daily dosing of chloroquine (B. Van Bonn, personal communication, May 2021). Moreover, drug degradation in circulating saltwater aquariums has become increasingly problematic as degradation of a similar anti-parasitic drug, praziquantel has been reported on multiple occasions [4]. Immediate water change after the disappearance of chloroquine at Shedd did not yield any improvement. Even if it had been effective, the practice of addressing undesirable chloroquine degradation using a water change to provide a system "reset" is resource-intensive and may not be feasible for larger exhibits which can contain millions of gallons of artificial saltwater [5].

Despite the existence of copper-based drugs, chloroquine phosphate is one of the few options available for treating *Cryptocaryon* outbreaks in large-scale aquarium habitats, as many marine animals, invertebrates, and fishes are sensitive to copper drugs at concentrations that are below therapeutic levels [6]. Additionally, many non-targeted microorganisms such as nitrifying bacteria will be negatively impacted by parasitic treatments that utilize copper. Thus, degradation of chloroquine severely limits available treatment options. As a result, it is critical to understand the contributors to the degradation process and reveal options to restore drug efficacy.

Prior studies have demonstrated the abiotic transformation of chloroquine under physical and chemical stresses (e.g., acid, alkaline, heat, light and oxidation) [7, 8] as well as in vitro chloroquine metabolism mediated by cytochrome P450 in mammalian cells [9]. However, the current understanding of chloroquine degradation in aquatic habitats is limited, and microbial degradation pathways specific to chloroquine have not been established in prokaryotic species. Chloroquine along with many other pharmaceuticals and personal care products (PPCPs) have become an emerging concern in the natural environment because of their ability to reach aquatic systems with sewage effluents [10, 11]. The Oslo-Paris Convention for the Protection of the Marine Environment of the North-East Atlantic (OSPAR) in the EU included chloroquine and chloroquine diphosphate as substances of possible concern in 2002 [10, 11]. Studying microbial chloroquine degradation and the environmental fate of chloroquine in saltwater aquariums is thus informative for aquarium management and for understanding phenomena that may occur in marine environments.

Here, we sought to characterize the microbial communities from saltwater aquarium systems recognized to degrade chloroquine and investigated the contribution of abiotic and microbially-mediated chloroquine degradation through analytical chemistry and metagenomic sequencing. Using statistical differential abundance analysis, we identified community members and functional genes associated with microbial chloroquine degradation in tropical saltwater systems. This study is the first to address the microbial degradation of chloroquine in marine systems and our findings will improve management practices that best support healthy animal populations in closed loop aquariums, as well as advancing our understanding of the microbial ecology of these specialized built environments.

2. Material and Methods

2.1. System Setup and Sampling Overview

Between November 2018 and 2020, samples were collected from multiple tropical saltwater aquariums extensively focusing on a behind-the-scenes quarantine system #3 (Q3) at Shedd Aquarium (Illinois, USA). Q3 is a 1500-gallon closed loop system composed of 17 tanks, one sump, and a series of water treatment units (Figure 1). Q3 was not inhabited by any marine animals during the sampling period and underwent a complete water change before the treatment in January 2020. To maintain the nitrifying microorganisms (e.g. ammonia-oxidizing bacteria, ammonia-oxidizing archaea, nitrite-oxidizing bacteria, etc.) in the biotower, either ammonium chloride solution or organic drip leftover from stingray food prep was used for continuous seeding of nitrogen. Chicago city water filtered through activated carbon units on site was mixed with Instant Ocean^{TM}, a commercial salt mix, in the sump before being distributed into individual tanks. After reaching the holding capacity on January 9th, no additional inflow was pumped into

the system until January 22nd. Due to evaporation and volume loss from continuous sampling, 80 gallons of artificial salt water were added to the sump on January 22nd. Prior to the chloroquine treatment conducted in January 2020, Q3 was treated with chloroquine on June 7th, 2019 (SI Figure 1) and did not exhibit severe drug degradation.

Samples were taken from tanks R1-R8 and the sump for ease of access. Chloroquine phosphate was dosed into the sump after pretreatment samples (PRE) were collected on January 9th. Decrease in chloroquine concentration was first observed on January 16th, therefore a set of samples (DEG1) were taken on January 17th to capture any changes associated with this transition. Before terminating the test run on January 27th, additional samples were taken on January 21st (DEG2). At each timepoint mentioned above, 2.05 L bulk water was collected from the sump and four out of the 17 tanks. Swabs from inlet and outlet PVC pipes were taken from tanks only. 2 L water was filtered through 0.22 µm polyethersulfone (PES) membrane onsite. 50 mL water samples, swabs, and filter membranes were stored at -20°C until use.

2.2. Bench-Scale Enrichment for Chloroquine-Degrading Microorganisms

To demonstrate the involvement of microbially-mediated degradation processes, bench-scale enrichment experiments were conducted in 40 mL artificial sea water (ASW) supplemented with 10 mg/L chloroquine phosphate to select for chloroquine-degrading microorganisms capable of using chloroquine as the sole carbon and nitrogen source for growth (SI Methods). Filter membranes and swabs collected on site were transferred into ASW enrichment culture and kept in the dark at 25 °C to avoid possible photodegradation. Controls for abiotic degradation were

included as well. Chloroquine concentration was measured every other day using a UV-Vis spectrophotometry protocol [12]. Enrichment samples were sub-cultured every nine days by mixing 10 mL current enrichment sample with 30 mL fresh ASW containing 10 mg/L chloroquine phosphate. In addition to Q3, tank/sump and pipeline swab samples were collected as in Q3 from two display exhibits (UB14: Underwater Beauty 14 and LM: Lagoon and Mangrove Forest) and included in this bench-scale enrichment study. More information on the ASW formulation and these two exhibits can be found in the SI.

2.3. DNA Extraction and Sequencing

Samples selected for metagenomic sequencing were collected during two sampling events (Q3: January 2020 and UB14: May 2019). Both initial and enrichment samples were included. All liquid samples were concentrated on PES 0.22 µm filters (Millipore Express Plus, MA) before DNA extraction, following the manufacturer's protocol of the MasterPure™ Complete DNA and RNA Purification Kit (Lucigen, WI). Library preparation and shotgun metagenomic sequencing were performed at the DNA Services (DNAS) facility of the Research Resources Center (RRC) at the University of Illinois at Chicago (UIC) using the Nextera DNA Flex Library Prep (Illumina, CA). In total, 57 libraries (54 biological samples and three kit/field blanks) were pooled and sequenced across two lanes using a NovaSeq6000 with 250 bp paired-end reads. Raw sequencing data has been deposited under NCBI BioProject PRJNA731192.

2.4. Microbiome Data Analysis

Raw sequences were trimmed using Kneaddata v0.7.10 (https://github.com/biobakery/kneaddata) to remove any field and/or human contaminants, adapters, and low-quality reads. Sample coverage was assessed using Nonpareil v3.304 [13]. To conduct genome-centric analysis, trimmed reads were assembled using metaSPAdes v3.14.1 [14]. Binning tools including CONCOCT v1.0.0 [15], MetaBAT2 v2.12.1 [16], MaxBin2 v2.2.6 [17], were used to reconstruct draft genomes from shotgun metagenomic assemblies. Metagenome-assembled genomes (MAGs) were dereplicated at 95% Average Nucleotide Identity (ANI) using deRep v2.6.2 [18]. Dereplicated bins were further refined, and quality-controlled using MetaWRAP v1.3.0 [19] and checkM v1.0.12 [20], respectively. Bins with greater than 50% completeness and less than 10% contamination were annotated using Prokka v1.14.6 [21]. KEGG [22], COG [23], and MetaCyc [24] databases were used for pathway reconstruction. Short reads were mapped onto draft bins using MetaWRAP v1.3.0 [19]. Comparative genomic analysis was conducted based on Amino Acid Identity (AAI) using CompareM v0.1.2 (https://github.com/dparks1134/CompareM). Taxonomic profiling of the dereplicated MAGs was determined primarily using PhyloPhlAn 3.0 [25]; results from Kaiju Web [26], GTDB-TK v1.4.0 [27], and MiCA Online [28] were also incorporated to better support taxonomic profiling of unknown features and resolve inconsistencies in taxonomic assignment across different tools. Due to the high percentage of unknown taxonomic classifications associated with environmental taxa that are often poorly characterized in existing databases (i.e. MetaPhlan3 [29] and Kraken2 [30]), taxonomic classifications of the dataset were conducted using Metaxa2 v2.2 [31] focusing on Small Subunit rRNA (i.e. 16S rRNA) filtered from the shotgun metagenomic libraries. Community functions and metabolic potentials were assessed using HUMAnN v3.0.0.alpha.3 [32].

2.5. Statistical Analysis

Differential abundance analyses were conducted focusing on Metaxa's taxonomic profile (relative abundance rarefied to the 15th percentile according to [33, 34]), MAG abundance (genome copies per million reads, CPM), and functional genes/pathways using MaAsLin2 linear model fitting with the following parameters: min_abundance = 0, min_prevalence = 0.1, normalization = TSS, transform = LOG, and standardize = TRUE [35]. Taxonomic features, MAGs, functional genes/pathways with a Benjamini-Hochberg adjusted p-value less than 0.05 were determined to be statistically significant. Covariates included in differential abundance analyses were determined using permutational multivariate analysis of variance (PERMANOVA). Variables with PERMANOVA (permutation 9,999) $p<0.05$ were considered as sources of variation. Other R packages (R version 4.0.4, 2021-02-15) used include phyloseq [36], vegan (https://github.com/vegandevs/vegan), and ggplot2 (https://github.com/tidyverse/ggplot2).

2.6. Liquid chromatography-mass spectrometry (LC-MS) Analysis

Liquid samples were filtered using 0.22 µm Target2™ Regenerated Cellulose Syringe Filters (ThermoFisher Scientific, MA) with quinine added as an internal standard. Following filtration, 0.5 µL samples were injected into a 2.1 mm x 50 mm Hypersil^{TM} BDS C_{18} column (ThermoFisher Scientific, MA) connected to a Bruker AmaZon-X Ion Trap Mass Spectrometer with a mobile phase consisting of 13% acetonitrile, 87% water, and 0.1% formic acid. Flow (0.3 mL/min) exiting the column in the first minute was diverted to waste, preventing highly soluble salt ions from entering the electron spray ionization (ESI) channel and causing ion suppression. MS detection was performed with positive mode ESI. Putative degradation products were identified based on the isotopic features of chlorine and carbon atoms. Selected samples were

submitted to the Integrated Molecular Structure Education and Research Center (IMSERC) at Northwestern University for accurate mass determination and formula verification of previously identified putative degradation products using an Agilent 6210 Time of Flight (TOF) Mass Spectrometer coupled with Agilent 1100 Series LC. Positive-ion spectra were collected under positive ESI and 2 GigHz detector mode. Data acquisition and analyses were done using the Agilent MassHunter Software. 5 µl/min methanol with 1% formic acid was used as the mobile phase and samples were analyzed with 2 µL direct loop injection.

3. Results and Discussion

3.1. Contribution of Microbially-Mediated Chloroquine Degradation Processes

Following a complete water replacement and stabilization of the system, the Q3 chloroquine treatment trial started on January 9, 2020. Chloroquine concentration dropped after seven days of gradual increase in chloroquine concentration (Figure 2). The contribution of microbially-mediated chloroquine degradation processes in Q3 was validated through a series of bench-scale enrichment experiments (Figure 3). Abiotic controls, kept in either dark or ambient light, did not show significant decrease in chloroquine concentration over 19 days. In Q3, decreases in chloroquine concentration primarily occurred in outlet swab samples and less prevalently in inlet samples, indicating that inlet and outlet microbial communities might be shaped differently (e.g. by differences in hydrodynamics characteristics such as flow turbulence). This observation was consistent across six out of the eight quarantine tanks, where water, inlet swab, and outlet swab were collected. The R4 and R6 tanks, operated at a higher flow rate compared to the other tanks, did not demonstrate evident chloroquine degradation.

Chloroquine degradation had previously been observed in the Q3 system, therefore it might have already been colonized by chloroquine-utilizing microbial communities. However, enrichment of DEG1 and DEG2 samples (samples collected after the occurrence of chloroquine degradation on site) exhibited an immediate decrease in chloroquine concentration, whereas enrichment of pretreatment samples (PRE) tended to require more time (paired student's t-test $p<0.05$ for PRE vs DEG1). This may indicate that the initial abundance of chloroquine-degrading microorganisms in PRE samples is lower compared to degradation samples (e.g. DGE1, and DEG2). In contrast, tank water and outlet swab samples collected in August 2019 from a studied exhibit system (LM), where chloroquine degradation did not occur on site, were able to maintain a stable chloroquine concentration throughout the enrichment period (SI Figure 2).

Consistent with previous Q3 observations that no chloroquine degradation was observed from water samples composed mainly of planktonic cells, an exhibit sampled in May 2019, Underwater Beauty 14 (UB14), also demonstrated the importance of pipeline (inlet and outlet) communities for chloroquine degradation (SI Figure 3). Therefore, water pipes may play an essential role in facilitating the attachment of chloroquine-degrading communities. The potential involvement of pipeline-attached biofilm in aquarium veterinary drug degradation has been also hypothesized [4]; praziquantel, a similar anti-parasite drug, was shown to degrade within marine aquariums during a typical 30-day treatment. Unoccupied systems treated with up to 200 ppm Cl^- for 24 hours still displayed praziquantel degradation within three days of treatment, likely due to slow or incomplete penetration of bleach within biofilms.

3.2. The Aquarium Microbiome

Trimming resulted in a total of 342 Gbp and 1,446 million high-quality reads with an average length of 237 bp. Estimated sequencing coverage ranged from 52.63% to 97.3% (n= 54; average = 82.38%, median = 85.94%, standard deviation = 11.14%) (SI Figure 4 and SI File 1). 16S rRNA reads extracted from the shotgun metagenomic dataset revealed 668 known microbial genera, belonging to 259 families, 133 orders, 60 classes, 30 phyla and 2 kingdoms after removing singletons (SI Figure 5). Prominent bacterial phyla in pipeline and tank water samples collected from Q3 and UB14, in descending average relative abundance, included *Proteobacteria*, *Actinobacteria*, *Bacteroidetes*, *Firmicutes*, *Planctomycetes*, *Cyanobacteria*, *Nitrospirae*, and *Chlamydiae* (Figure 4A and Figure 4B). Archaeal phylum *Thaumarchaeota* was also detected in relatively high abundance and frequencies. Comparing the alpha diversity indices (Chao1, observed species, Shannon and Simpson diversity indices) of the unoccupied aquarium (Q3) to UB14, which served as the habitat of eight marine species (details listed in SI), statistical testing showed no significant difference for all indices (SI Figure 6; Wilcox's $p > 0.05$). Outlet samples were shown to have greater species richness (Chao1 and observed) than inlet samples (Wilcox's $p < 0.05$). Meanwhile, Shannon and Simpson diversity indices of outlet microbial communities were significantly higher (Wilcox's $p < 0.05$ for Shannon and Wilcox's $p < 0.01$ for Simpson) than tank water microbiomes.

Based on nonmetric multidimensional scaling analysis, microbial communities cluster by aquarium (Q3 vs UB14; PERMANOVA 9,999 permutation $R^2 = 0.07$, $p = 0.0009$), despite the similarities in alpha-diversity (Figure SI 5 and Figure 4D). Within each aquarium, inlet and outlet microbiome compositions overlapped more compared to tank water (location:

PERMANOVA $R^2 = 0.1$, $p = 0.0134$). Furthermore, Q3 samples collected before- and after-dosing (Figure 4E) demonstrated compositional changes following chloroquine dosing across sampling locations; compared to inlet and tank water samples, outlet microbial communities show the least amount of variation in microbial community and remained highly stable (location: $R^2 = 0.58$, $p = 0.0003$; collection time: $R^2 = 0.11$, $p = 0.06$). Q3 inlet samples collected before chloroquine dosing were uniquely inhabited by *Cyanobacteria*, whose relative abundance quickly declined following chloroquine dosing. This change was not observed from any other locations within Q3. From a genome-centric approach, a total of 754 dereplicated metagenome-assembled genomes (MAGs, < 95% ANI) were recovered from this dataset (>50% completeness and <10% contamination). 745 were assigned to bacterial genomes, with the remaining nine assigned as archaea. 500 of the bacterial genomes belong to the phylum of *Proteobacteria* and the five most prevalent phyla include *Proteobacteria*, *Bacteroidetes*, *Actinobacteria*, *Firmicutes*, and *Cyanobacteria*. The five MAGs detected with the highest copy numbers were 1) *Thalassobaculum litoreum*, 2) *Gordonia* sp MMS17 SY073, 3) *Nitratireductor* sp StC3, 4) *Altermonas flava*, and 5) *Leisingera* sp ANG1. This taxonomic classification aligns well with the previous 16S rRNA-based taxonomic profiling (Figure 4A & 4B).

3.3. Differentially Abundant Taxa, MAGs, and Metabolic Potentials

511 out of the 754 dereplicated MAGs were detected in both Q3 and UB14 samples, whereas 151 and 92 MAGs were unique to Q3 and UB14, respectively. Furthermore, 241 core MAGs were detected from more than 75% of the aquarium samples (41 samples or more) and 357 rare MAGs were identified from less than 50% of the samples (26 samples or less). Seven microbial taxa resolved at genus level and 21 MAGs (SI File 2) were significantly enriched (FDR < 0.05)

in samples where chloroquine degradation was observed during bench-scale enrichment, compared to those where chloroquine degradation was not observed (Figure 5). The majority of the features were taxonomically assigned to phyla *Actinobacteria*, *Bacteroidetes*, *Chloroflexi*, and *Proteobacteria*, among which *Nitratireductor* and *Nitrospira* (Q3-DEG1-R6OUT-BIN38) represented the feature with the greatest effect size (coefficient) in short-read-based and genome-centric analyses, respectively. The MAG of *Nitrospira* contains several annotated genes related to nitrate and nitrite reduction (*nirD*, *nirK*, *narG*, *narZ*, *nxrA*, *narH*, *narY*, and *nxrB*; SI File 3).

Chemical analysis (Section 4.4 below) suggested that the microbial degradation of chloroquine involved deamination on the alkyl side chain, releasing both carbon and nitrogen into the nutrient- and ammonia-limited system. Indeed, MAGs and taxa present at high relative abundance in degradation samples (e.g. outlet samples taken from tank R1 and R2) were predicted able to utilize a diverse range of carbon sources for growth, such as starch-degrading *Sandaracinus amylolyticus* (Q3-DEG2-R1OUTLET-BIN60) [37, 38], as well as *Cellulomonas* (Q3-PRE-R4OUTLET-BIN19) with high amylase, cellulase and xylanase activities [39].

Additionally, differential analysis focusing on Q3 outlet samples (R4 and R6 vs R1 and R2) revealed that *Polyangiaceae* were present at higher relative abundance in outlet samples where chloroquine degradation occurred during enrichment compared to those where chloroquine concentration was stable. Although lacking resolution to further taxonomically assign genus and/or species identification, bacteria belonging to the family of *Polyangiaceae* have been either directly shown to be cellulose-, agar-, and toluene-degraders [40, 41] or significantly enriched in

activated sludges receiving wastewater containing petroleum products [42] and BTEX (benzene, toluene, ethyl benzene, and xylene) [43].

In addition to bacteria associated with diverse carbon metabolic strategies, a large proportion of differentially abundant features have important ecological functions in nitrogen cycling; particularly, *Nitratireductor*, along with many genera and species belong to the order of *Rhizobiales*, are capable of reducing nitrate into nitrite. Few isolated strains were shown to reduce nitrite into nitrous oxide for energy production [44-46]. Nitrate is a pollutant that accumulates quickly in closed systems, such as marine aquariums, but considered less toxic compared to ammonia and nitrite [47, 48]. It is usually removed biologically in an anerobic denitrification system, where oxygen is replaced by nitrate as an electron acceptor in bacterial respiration, or more commonly through complete or partial water changes. Although the tank water was constantly aerated, there may exist microaerobic or anoxic environments within biofilms where nitrate reduction can occur, since according to existing studies, mature biofilms can be mostly anaerobic, and oxygen can only penetrate approximately 50 μm below the oxic-anoxic interface given a 210 μm thick biofilm [49].

In conjunction with microbial community members present at differential relative abundance, we assessed the metabolic potentials of the aquarium microbial community using HUMANN3 and MaAsLin2 linear model fitting, focusing on MetaCyc Pathway definitions (Figure 6). Several pathways related to denitrification (e.g. nitrate reduction I, nitrifier denitrification) were enriched in samples where bench-scale chloroquine degradation was reported (FDR < 0.05). KEGG

Orthologs (KO) belonging to these pathways, including nitrate reductase (FDR = 0.023), and nitrite reductase (FDR = 0.011), have significantly higher copy numbers in degradation samples. Other pathways corresponding to the superclass of polyamine degradation (i.e., phenylethylamine degradation, and phenylacetate degradation) were associated with chloroquine-degrading communities as well. Future transcriptomic studies can further substantiate our findings and advance our understanding of the aquarium microbiome in relation to veterinary drug degradation.

3.4. Identification of Putative Microbially-Mediated Chloroquine Degradation Products

From LC-LRMS, two potential degradation products, *m/z* 279.05 and *m/z* 265.07 (SI Figure 7), were identified from multiple Q3 and enrichment samples. No degradation products were found from abiotic control samples. To further confirm the identity of these degradation products, HR-MS yielded accurate masses of *m/z* 279.0895 and *m/z* 265.1103, which most likely match with the protonated adduct of $C_{14}H_{15}ClN_2O_2$ (278.082205 g/mol) and $C_{14}H_{17}ClN_2O$ (264.102941 g/mol) at a precision of 0.02 mDa, respectively. Putative structures for the above chemicals (SI Figure 8), developed based on structural similarity and previous literature on chloroquine metabolism, support the hypothesis that chloroquine degradation is linked to N utilization.

Few studies have addressed the microbial degradation of chloroquine in aquatic environments as the majority of the studies have focused on abiotic degradation of chloroquine under physical and chemical stresses (e.g. acid, alkaline, heat, light and oxidation) [7, 8], as well as in vitro chloroquine metabolism mediated by cytochrome P450 in mammalian cells [9]. Despite the

existence of established pathways of aromatic amine degradation, the quinoline ring of chloroquine is believed to be resistant to most abiotic and biotic degradations [50-52]. This is in good agreement with the two degradation products detected in the saltwater aquariums; likewise for metabolic products associated with cytochrome P450 (CYPS) proteins (e.g. desethyl chloroquine and bisdesethyl chloroquine), modifications are mostly associated with the alkyl side chain [51, 52]. Consistent with our HR-MS results, early studies on drug metabolism have also identified 4-[(7-chloroquinolin-4-yl)amino]pentanoic acid ($C_{14}H_{15}ClN_2O_2$) from both human plasma [53] and urine [54] samples (SI Figure 8). Furthermore, the involvement of enzymatic deamination in drug metabolism has been demonstrated by other of xenobiotic drugs structurally similar to chloroquine; for example, a dimethylamino and a diethylamino group were separated from diphenhydramine and metoclopramide, respectively [55-57].

In systems where ammonia is tightly controlled (i.e. Q3), microbial deamination and utilization of organic nitrogen may alleviate the shortage of nitrogen and carbon simultaneously, potentially providing essential elements for nitrogen assimilation and amino acid synthesis. On the other hand, the cellulose- and polysaccharide-degrading microorganisms preciously discussed in Section 4.3 may indirectly relate to the deamination of chloroquine as nitrogen source and availability have important implications on cellulose and polysaccharide degradation [58, 59]. *Bacillus subtilis* isolated from environmental samples rich in cellulose displayed the highest activity of cellulose-degrading enzymes when a 1:1 ratio of organic and inorganic nitrogen mixture was supplied [59]. In contrast, *Phanerochaete chrysosporium* was found to degrade cellulose faster with organic nitrogen sources compared to inorganic NH_4Cl [58]. While nitrogen uptake preferences are different across different microorganisms, degradation of chloroquine

may alter aquariums' nitrogen availability, and potentially facilitate the increase in relative abundance of cellulose-degrading microorganisms. Interestingly, an outlet sample plated on solidified artificial saltwater agar with chloroquine (10 mg/L) displayed a pitting morphotype. This morphological feature suggestive of agar degradation was not found on artificial saltwater agar plates without chloroquine (SI Figure 9), supporting the importance of chloroquine as a nitrogen source for cellulose-degraders.

3.5. Practical Implications on Managing Veterinary Drug Degradation in Saltwater Aquariums

Although our results indicated the importance of nitrogen management in relation to chloroquine degradation in circulating saltwater aquariums, alteration of current nitrogen management practices is impractical, considering the acute toxicity of ammonia and nitrite for aquatic animals. Being able to maintain an aquarium with ammonia and nitrite concentrations as close to zero as possible remains one of the most essential animal health objectives.

Meanwhile, our enrichment results highlight the importance of pipeline-associated microorganisms in microbial chloroquine degradation. Outlet samples collected from tank R4 and R6, which were operated at a slightly higher flow rate, did not demonstrate significant chloroquine degradation during enrichment. Furthermore, in Q3, chloroquine degradation was primarily localized within outlet pipes not inlet, likely due to differences in hydrodynamic characteristics at the sampling locations. Flow velocity, along with other factors such as pipe materials, biodegradable organic matter, and disinfectants, have been shown to profoundly influence the formation and development of biofilms [60, 61]. Since many hydrodynamic conditions studied previously might not be directly applicable for aquarium management from an animal

health perspective (e.g., overly-high flow rates can exhaust small-bodied fish), aquarium trials under conditions that reflect specific needs of the animals will be beneficial to prevent or delay the attachment of chloroquine-degrading microorganisms to pipeline surfaces.

For systems that continuously experienced drug degradation, chemical removal of chloroquine-degrading microbial communities remains challenging. In an attempt to mitigate microbial degradation of praziquantel in saltwater aquariums, bleach cleaning with up to 200 ppm Cl^- did not yield notable improvements [4], which is likely a result of restricted penetration of disinfectant through the extracellular polymeric substance (EPS) of biofilms [62]. Microorganisms that survived the chemical cleaning could also participate in redispersal and subsequent recolonization of the system [4, 63]. If chemical removal is preferred, selection of disinfectants, concentration, and exposure time need to be examined with precautions to avoid phenotypic adaptations of biofilm cells to sublethal concentrations of disinfectants. Alternatively, depending on system design, physical removal of biofilms may be feasible especially for pipes directly connected to inlets and outlets.

4. Conclusions

We incorporated a metagenomic approach with analytical chemistry to investigate the microbial contribution to veterinary drug degradation which occurred in Shedd's tropical saltwater aquariums. Through a series of bench-scale enrichment experiments, we showed that the chloroquine-degrading communities were primarily localized within system pipelines. Depending on specific hydrodynamic characteristics (e.g., flow rate, turbulence) unique to each

system, chloroquine-utilizing microorganisms may colonize outlet and/or inlet pipes. Although chloroquine dosing caused structural and compositional differences between pre- and post-dosing samples, aquarium microbiomes mainly reflected sampling location. Samples enriched with chloroquine-degrading microorganisms contained higher proportions of microbial taxa and MAGs with diverse carbon and nitrogen metabolism capabilities. Overall, our results expand the body of knowledge surrounding aquarium microbiomes and veterinary drug degradation, revealing how microbial ecology and chemistry can be integrated into future management of saltwater circulating enclosures. Furthermore, these findings might illuminate phenomena occurring in other nitrogen-limited environments when nitrogen-containing anthropogenic chemicals are added.

5. Acknowledgement

This project was supported in part by the Searle Leadership Fund and by the Helen V. Brach Foundation. J.H. was supported by a Terminal Year Fellowship from the McCormick School of Engineering and Applied Science. We gratefully acknowledge the following people for their support, without whose help this work would never have been possible: Tiffany Adams, Stephanie Goehring, Sage Butts, Allen LaPointe, Dr. Lee Pinnell, Kurt Hettiger, Kayla Melton and Shedd volunteers. This work made use of the IMSERC MS facility at Northwestern University, which has received support from the Soft and Hybrid Nanotechnology Experimental (SHyNE) Resource (NSF ECCS-2025633), and Northwestern University. Sequencing was performed at the DNA Services (DNAS) facility within the Research Resources Center (RRC) at the University of Illinois at Chicago (UIC).

This research was supported in part through the computational resources and staff contributions provided by the Genomics Compute Cluster which is jointly supported by the Feinberg School of Medicine, the Center for Genetic Medicine, and Feinberg's Department of Biochemistry and Molecular Genetics, the Office of the Provost, the Office for Research, and Northwestern Information Technology. The Genomics Compute Cluster is part of Quest, Northwestern University's high performance computing facility, with the purpose to advance research in genomics.

6. Conflict of interest

The authors declare that they have no conflict of interest.

7. Figure Captions

Figure 1 Quarantine System 3 (Q3) Set-up. Tanks R1, R2, and R3 each have a maximum holding capacity of 110.4 gal; tanks R5, R6, R7, and R8, 91.7 gal; R4, R9, R10, R11, R12, R14, R15, R16, R17, 53.5 gal. Sump has a holding capacity between 75 and 104 gal. Sampling primarily focused on tanks R1-8 for ease of access; therefore, tanks R9-17 were omitted from the diagram for simplicity. All tanks were continuously aerated during the operation. The system is also equipped with a UV sterilizer that was not in use at the time of sample collection, therefore excluded from the above diagram. During the January 2020 sampling period, R4 and R6 were operated at a higher flow rate than the rest of the Q3 tanks.

Figure 2 Water quality measurements (temperature, pH, salinity, ammonia, nitrite, and nitrate), chloroquine dosing (g), chloroquine concentration (mg/L) measured on-site using a UV-Vis spectrophotometer, and expected chloroquine concentration (mg/L) calculated based on daily chloroquine addition and concentration measurements between January 9th and January 27th, 2020. Nitrate and nitrite were measured once per week, whereas other water quality metrics were monitored daily.

Figure 3 Chloroquine concentration of enrichment cultures seeded with PRE (A), DEG1 (B), and DEG2 (C) samples collected from eight tanks (R1-8) and the sump. Abiotic controls were kept either under ambient light or in dark along with aquarium samples for 19 days. Color corresponds to the sample type/location.

Figure 4 Taxonomic composition, alpha-, and beta-diversity of the saltwater aquarium microbiomes. Phylum-level microbial composition of 18 tank water and swab samples (un-enriched) collected from Q3 (A) and UB14 (B); a complete taxonomic compositional plot including all 54 samples can be found in SI Figure 5. Alpha-diversity indices (Chao1, Observed, Shannon, and Simpson) of 46 samples after rarefication (C). Bray-Curtis based non-metric multidimensional scaling (NMDS) of 46 rarefied samples (D) and 12 Q3 samples collected before and after chloroquine dosing (E). Significance level: ** $p < 0.01$; * $p < 0.05$.

Figure 5 Differentially abundant (relative abundance) genera (A) and metagenome-assembled genomes (B) detected using MaAsLin2's linear model fitting. Large dots correspond to the

average log_{10} values of samples belonging to each group (N – significant chloroquine degradation not observed from bench-scale enrichment experiments and Y - chloroquine concentration decrease observed from bench-scale enrichment experiments). Taxonomic classification of the 21 differentially abundant MAGs was manually curated by incorporating results from Kaiju [26], GTDB-TK [27], Phylophlan [25], and MiGA [28]. Significance level: *** $p < 0.001$; ** $p < 0.01$; * $p < 0.05$.

Figure 6 Relative abundance in log_{10}(CPM) (copies per million reads) of differential abundant pathways based on MetaCyc definitions. Differentially abundant pathways were determined using MaAsLin2 linear model fitting with FDR < 0.05. Coefficients indicate the contrast between samples where chloroquine degradation was observed during enrichment and those where chloroquine degradation did not occur. A greater coefficient corresponds to a higher effect size. Significance level: *** $p < 0.001$; ** $p < 0.01$; * $p < 0.05$.

8. Reference

1. Leethochavalit, S., *Characterization of Cryptocaryon sp. isolated from marine fish in Thailand and in vitro treatment*. 2011.

2. Colorni, A.; Burgess, P., Cryptocaryon irritans Brown 1951, the cause of 'white spot disease' in marine fish: an update. *Aquarium Sciences and Conservation* **1997,** *1*, 217-238.

3. Van, K.; Doan, N., The prevalence of Cryptocaryon irritans in wild marine ornamental fish from Vietnam. *IOP Conference Series: Earth and Environmental Science* **2018,** *137*, 012094.

4. Thomas, A.; Dawson, M. R.; Ellis, H.; Stamper, M., Praziquantel degradation in marine aquarium water. *PeerJ* **2016,** *4*.

5. Patin, N. V.; Pratte, Z. A.; Regensburger, M.; Hall, E.; Gilde, K.; Dove, A. D. M.; Stewart, F. J., Microbiome dynamics in a large artificial seawater aquarium. *Applied and Environmental Microbiology* **2018,** *84* (10), e00179-18.

6. Cardeilhac, P. T.; Whitaker, B. R., Copper treatments: Uses and precautions. *Veterinary Clinics of North America: Small Animal Practice* **1988,** *18* (2), 435-448.

7. Coelho, A. S.; Chagas, C. E. P.; de Pádua, R. M.; Pianetti, G. A.; Fernandes, C., A comprehensive stability-indicating HPLC method for determination of chloroquine in active pharmaceutical ingredient and tablets: Identification of oxidation impurities. *Journal of Pharmaceutical and Biomedical Analysis* **2017,** *145*, 248-254.

8. Doddaga, S.; Peddakonda, R., Chloroquine-N-oxide, a major oxidative degradation product of chloroquine: Identification, synthesis and characterization. *Journal of Pharmaceutical and Biomedical Analysis* **2013,** *81-82*, 118-125.

9. Projean, D.; Baune, B.; Farinotti, R.; Flinois, J.-P.; Beaune, P.; Taburet, A.-M.; Ducharme, J., In vitro metabolism of chloroquine: identification of CYP2C8, CYP3A4, and

CYP2D6 as the main isoforms catalyzing N-desthylchloroquine formation. *Drug Metabolism and Disposition* **2003,** *31* (6), 748.

10. McEniff, G.; Schmidt, W.; Quinn, B., Pharmaceuticals in the aquatic environment: a short summary of current knowledge and the potential impacts on aquatic biota and humans. **2015**.

11. Roberts, P. H.; Bersuder, P., Analysis of OSPAR priority pharmaceuticals using high-performance liquid chromatography-electrospray ionisation tandem mass spectrometry. *Journal of Chromatography A* **2006,** *1134* (1), 143-150.

12. Takla, P. G.; Dakas, C. J., A study of interactions of chloroquine with ethanol, sugars and glycerol using ultraviolet spectrophotometry. *International Journal of Pharmaceutics* **1988,** *43* (3), 225-232.

13. Rodriguez-R, L. M.; Gunturu, S.; Tiedje, J. M.; Cole, J. R.; Konstantinidis, K. T., Nonpareil 3: Fast estimation of metagenomic coverage and sequence diversity. *mSystems* **2018,** *3* (3), e00039-18.

14. Nurk, S.; Meleshko, D.; Korobeynikov, A.; Pevzner, P. A., metaSPAdes: a new versatile metagenomic assembler. *Genome research* **2017,** *27* (5), 824-834.

15. Alneberg, J.; Bjarnason, B. S.; de Bruijn, I.; Schirmer, M.; Quick, J.; Ijaz, U. Z.; Lahti, L.; Loman, N. J.; Andersson, A. F.; Quince, C., Binning metagenomic contigs by coverage and composition. *Nature Methods* **2014,** *11* (11), 1144-1146.

16. Kang, D. D.; Li, F.; Kirton, E.; Thomas, A.; Egan, R.; An, H.; Wang, Z., MetaBAT 2: an adaptive binning algorithm for robust and efficient genome reconstruction from metagenome assemblies. *PeerJ* **2019,** *7*, e7359-e7359.

17. Wu, Y.-W.; Simmons, B. A.; Singer, S. W., MaxBin 2.0: an automated binning algorithm to recover genomes from multiple metagenomic datasets. *Bioinformatics* **2016,** *32* (4), 605-607.

18. Olm, M. R.; Brown, C. T.; Brooks, B.; Banfield, J. F., dRep: a tool for fast and accurate genomic comparisons that enables improved genome recovery from metagenomes through de-replication. *The ISME Journal* **2017,** *11* (12), 2864-2868.

19. Uritskiy, G. V.; DiRuggiero, J.; Taylor, J., MetaWRAP—a flexible pipeline for genome-resolved metagenomic data analysis. *Microbiome* **2018,** *6* (1), 158.

20. Parks, D. H.; Imelfort, M.; Skennerton, C. T.; Hugenholtz, P.; Tyson, G. W., CheckM: assessing the quality of microbial genomes recovered from isolates, single cells, and metagenomes. *Genome research* **2015,** *25* (7), 1043-1055.

21. Seemann, T., Prokka: rapid prokaryotic genome annotation. *Bioinformatics* **2014,** *30* (14), 2068-2069.

22. Kanehisa, M.; Goto, S., KEGG: Kyoto Encyclopedia of Genes and Genomes. *Nucleic Acids Research* **2000,** *28* (1), 27-30.

23. Tatusov, R. L.; Galperin, M. Y.; Natale, D. A.; Koonin, E. V., The COG database: a tool for genome-scale analysis of protein functions and evolution. *Nucleic acids research* **2000,** *28* (1), 33-36.

24. Caspi, R.; Billington, R.; Fulcher, C. A.; Keseler, I. M.; Kothari, A.; Krummenacker, M.; Latendresse, M.; Midford, P. E.; Ong, Q.; Ong, W. K.; Paley, S.; Subhraveti, P.; Karp, P. D., The MetaCyc database of metabolic pathways and enzymes. *Nucleic Acids Research* **2017,** *46* (D1), D633-D639.

25. Asnicar, F.; Thomas, A. M.; Beghini, F.; Mengoni, C.; Manara, S.; Manghi, P.; Zhu, Q.; Bolzan, M.; Cumbo, F.; May, U.; Sanders, J. G.; Zolfo, M.; Kopylova, E.; Pasolli, E.; Knight, R.; Mirarab, S.; Huttenhower, C.; Segata, N., Precise phylogenetic analysis of microbial isolates and genomes from metagenomes using PhyloPhlAn 3.0. *Nat Commun* **2020,** *11* (1), 2500.

26. Menzel, P.; Ng, K. L.; Krogh, A., Fast and sensitive taxonomic classification for metagenomics with Kaiju. *Nature Communications* **2016,** *7* (1), 11257.

27. Chaumeil, P.-A.; Mussig, A. J.; Hugenholtz, P.; Parks, D. H., GTDB-Tk: a toolkit to classify genomes with the Genome Taxonomy Database. *Bioinformatics* **2020,** *36* (6), 1925-1927.

28. Rodriguez-R, L. M.; Gunturu, S.; Harvey, W. T.; Rosselló-Mora, R.; Tiedje, J. M.; Cole, J. R.; Konstantinidis, K. T., The Microbial Genomes Atlas (MiGA) webserver: taxonomic and gene diversity analysis of Archaea and Bacteria at the whole genome level. *Nucleic Acids Research* **2018,** *46* (W1), W282-W288.

29. Beghini, F.; McIver, L. J.; Blanco-Míguez, A.; Dubois, L.; Asnicar, F.; Maharjan, S.; Mailyan, A.; Thomas, A. M.; Manghi, P.; Valles-Colomer, M.; Weingart, G.; Zhang, Y.; Zolfo, M.; Huttenhower, C.; Franzosa, E. A.; Segata, N., Integrating taxonomic, functional, and strain-level profiling of diverse microbial communities with bioBakery 3. *bioRxiv* **2020**, 2020.11.19.388223.

30. Wood, D. E.; Lu, J.; Langmead, B., Improved metagenomic analysis with Kraken 2. *Genome Biology* **2019,** *20* (1), 257.

31. Bengtsson-Palme, J.; Hartmann, M.; Eriksson, K. M.; Pal, C.; Thorell, K.; Larsson, D. G.; Nilsson, R. H., METAXA2: improved identification and taxonomic classification of small and large subunit rRNA in metagenomic data. *Mol Ecol Resour* **2015,** *15* (6), 1403-14.

32. Franzosa, E. A.; McIver, L. J.; Rahnavard, G.; Thompson, L. R.; Schirmer, M.; Weingart, G.; Lipson, K. S.; Knight, R.; Caporaso, J. G.; Segata, N.; Huttenhower, C., Species-level functional profiling of metagenomes and metatranscriptomes. *Nature Methods* **2018,** *15* (11), 962-968.

33. McMurdie, P. J.; Holmes, S., Waste not, want not: Why rarefying microbiome data ss inadmissible. *PLOS Computational Biology* **2014,** *10* (4), e1003531.

34. Weiss, S. J.; Xu, Z.; Amir, A.; Peddada, S.; Bittinger, K.; Gonzalez, A.; Lozupone, C.; Zaneveld, J. R.; Vazquez-Baeza, Y.; Birmingham, A.; Knight, R., Effects of library size variance, sparsity, and compositionality on the analysis of microbiome data. *PeerJ PrePrints* **2015,** *3*, e1157v1.

35. Mallick, H.; Rahnavard, A.; McIver, L. J.; Ma, S.; Zhang, Y.; Nguyen, L. H.; Tickle, T. L.; Weingart, G.; Ren, B.; Schwager, E. E.; Chatterjee, S.; Thompson, K. N.; Wilkinson, J. E.; Subramanian, A.; Lu, Y.; Waldron, L.; Paulson, J. N.; Franzosa, E. A.; Bravo, H. C.; Huttenhower, C., Multivariable association discovery in population-scale meta-omics studies. *bioRxiv* **2021**, 2021.01.20.427420.

36. McMurdie, P. J.; Holmes, S., Phyloseq: An R package for reproducible interactive analysis and graphics of microbiome census data. *PLoS One* **2013,** *8* (4), e61217.

37. Sharma, G.; Khatri, I.; Subramanian, S., Complete genome of the starch-degrading myxobacteria Sandaracinus amylolyticus DSM 53668T. *Genome biology and evolution* **2016,** *8* (8), 2520-2529.

38. Mohr, K. I.; Garcia, R. O.; Gerth, K.; Irschik, H.; Müller, R., Sandaracinus amylolyticus gen. nov., sp. nov., a starch-degrading soil myxobacterium, and description of

Sandaracinaceae fam. nov. *International journal of systematic and evolutionary microbiology* **2012,** *62* (5), 1191-1198.

39. Rajoka, M. I.; Malik, K. A., Cellulomonas. In *Encyclopedia of Food Microbiology*, Robinson, R. K., Ed. Elsevier: Oxford, 1999; pp 365-371.

40. Garcia, R.; Müller, R., Metagenomic approach for the isolation and cultivation of cellulose-degrading myxobacteria.

41. Laban, N. A.; Dao, A.; Foght, J., DNA stable-isotope probing of oil sands tailings pond enrichment cultures reveals different key players for toluene degradation under methanogenic and sulfidogenic conditions. *FEMS Microbiology Ecology* **2015,** *91* (5).

42. Shchegolkova, N. M.; Krasnov, G. S.; Belova, A. A.; Dmitriev, A. A.; Kharitonov, S. L.; Klimina, K. M.; Melnikova, N. V.; Kudryavtseva, A. V., Microbial community structure of activated sludge in treatment plants with different wastewater compositions. *Frontiers in Microbiology* **2016,** *7* (90).

43. Huang, Y.; Li, L., Biodegradation characteristics of naphthalene and benzene, toluene, ethyl benzene, and xylene (BTEX) by bacteria enriched from activated sludge. *Water Environment Research* **2014,** *86* (3), 277-284.

44. Labbé, N.; Parent, S.; Villemur, R., Nitratireductor aquibiodomus gen. nov., sp. nov., a novel α-proteobacterium from the marine denitrification system of the Montreal Biodome (Canada). *International Journal of Systematic and Evolutionary Microbiology* **2004,** *54* (1), 269-273.

45. Lai, Q.; Yu, Z.; Wang, J.; Zhong, H.; Sun, F.; Wang, L.; Wang, B.; Shao, Z., Nitratireductor pacificus sp. nov., isolated from a pyrene-degrading consortium. *International Journal of Systematic and Evolutionary Microbiology* **2011,** *61* (6), 1386-1391.

46. Lai, Q.; Yu, Z.; Yuan, J.; Sun, F.; Shao, Z., Nitratireductor indicus sp. nov., isolated from deep-sea water. *Int J Syst Evol Microbiol* **2011,** *61* (Pt 2), 295-298.

47. Soucek, D. J.; Dickinson, A., Acute toxicity of nitrate and nitrite to sensitive freshwater insects, mollusks, and a crustacean. *Archives of Environmental Contamination and Toxicology* **2012,** *62* (2), 233-242.

48. Tilak, K.; Veeraiah, K.; Raju, J. M. P., Effects of ammonia, nitrite and nitrate on hemoglobin content and oxygen consumption of freshwater fish, Cyprinus carpio (Linnaeus). *Journal of Environmental Biology* **2007,** *28* (1), 45-47.

49. Borriello, G.; Werner, E.; Roe, F.; Kim, A. M.; Ehrlich, G. D.; Stewart, P. S., Oxygen limitation contributes to antibiotic tolerance of Pseudomonas aeruginosa in biofilms. *Antimicrobial agents and chemotherapy* **2004,** *48* (7), 2659-2664.

50. Nord, K.; Karlsen, J.; Tønnesen, H. H., Photochemical stability of biologically active compounds. IV. Photochemical degradation of chloroquine. *International Journal of Pharmaceutics* **1991,** *72* (1), 11-18

51. Browning, D. J., Pharmacology of chloroquine and hydroxychloroquine. In *Hydroxychloroquine and Chloroquine Retinopathy*, Browning, D. J., Ed. Springer New York: New York, NY, 2014; pp 35-63.

52. Salako, L. A., Pharmacokinetics of antimalarial drugs: their therapeutic and toxicological implications. *Annali dell'Istituto superiore di sanita* **1985,** *21* (3), 315.

53. Tariq, M.; Al-Badr, A. A., Chloroquine. In *Analytical profiles of drug substances*, Elsevier: 1984; Vol. 13, pp 95-125.

54. Brown, N. D.; Poon, B. T.; Phillips, L. R., Identification and determination of a carboxylic acid metabolite of chloroquine in human urine by high-performance liquid

chromatography. *Journal of Chromatography B: Biomedical Sciences and Applications* **1989,** *487*, 189-196.

55. Argikar, U. A.; Gomez, J.; Ung, D.; Parkman, H. P.; Nagar, S., Identification of novel metoclopramide metabolites in humans: In vitro and in vivo studies. *Drug Metabolism and Disposition* **2010,** *38* (8), 1295.

56. Akutsu, T.; Kobayashi, K.; Sakurada, K.; Ikegaya, H.; Furihata, T.; Chiba, K., Identification of human cytochrome P450 isozymes involved in diphenhydramine N-demethylation. *Drug Metabolism and Disposition* **2007,** *35* (1), 72.

57. Baldacci, A.; Prost, F.; Thormann, W., Identification of diphenhydramine metabolites in human urine by capillary electrophoresis-ion trap-mass spectrometry. *Electrophoresis* **2004,** *25* (10-11), 1607-1614.

58. Reid, I. D., Effects of nitrogen sources on cellulose and synthetic lignin degradation by phanerochaete chrysosporium. *Applied and environmental microbiology* **1983,** *45* (3), 838-842.

59. Wita, A.; Białas, W.; Wiśniewska, R.; Szychowska, K.; Czaczyk, K., The influence of temperature and nitrogen source on cellulolytic potential of microbiota isolated from natural environment. *Pol J Microbiol* **2019,** *68* (1), 105-114.

60. Lehtola, M. J.; Laxander, M.; Miettinen, I. T.; Hirvonen, A.; Vartiainen, T.; Martikainen, P. J., The effects of changing water flow velocity on the formation of biofilms and water quality in pilot distribution system consisting of copper or polyethylene pipes. *Water Research* **2006,** *40* (11), 2151-2160.

61. Ollos, P. J.; Huck, P. M.; Slawson, R. M., Factors affecting biofilm accumulation in model distribution systems. *Journal AWWA* **2003,** *95* (1), 87-97.

62. Verderosa, A. D.; Totsika, M.; Fairfull-Smith, K. E., Bacterial biofilm eradication agents: A current review. *Frontiers in Chemistry* **2019,** *7* (824).

63. Solano, C.; Echeverz, M.; Lasa, I., Biofilm dispersion and quorum sensing. *Curr Opin Microbiol* **2014,** *18*, 96-104.

Credit Author Statement

Jinglin Hu: Conceptualization, Methodology, Formal analysis, Investigation, Writing, Editing, and Visualization

Nancy Hellgeth: Investigation and Editing

Chrissy Cabay: Resources, Funding Acquisition, and Editing

James Clark: Resources and Editing

Francis J. Oliaro: Resources and Editing

William Van Bonn: Resources and Editing

Erica M. Hartmann: Conceptualization, Funding Acquisition, Editing, and Supervision

Declaration of competing interests

☒ The authors declare that they have no known competing financial interests or personal relationships that could have appeared to influence the work reported in this paper

Figure 1

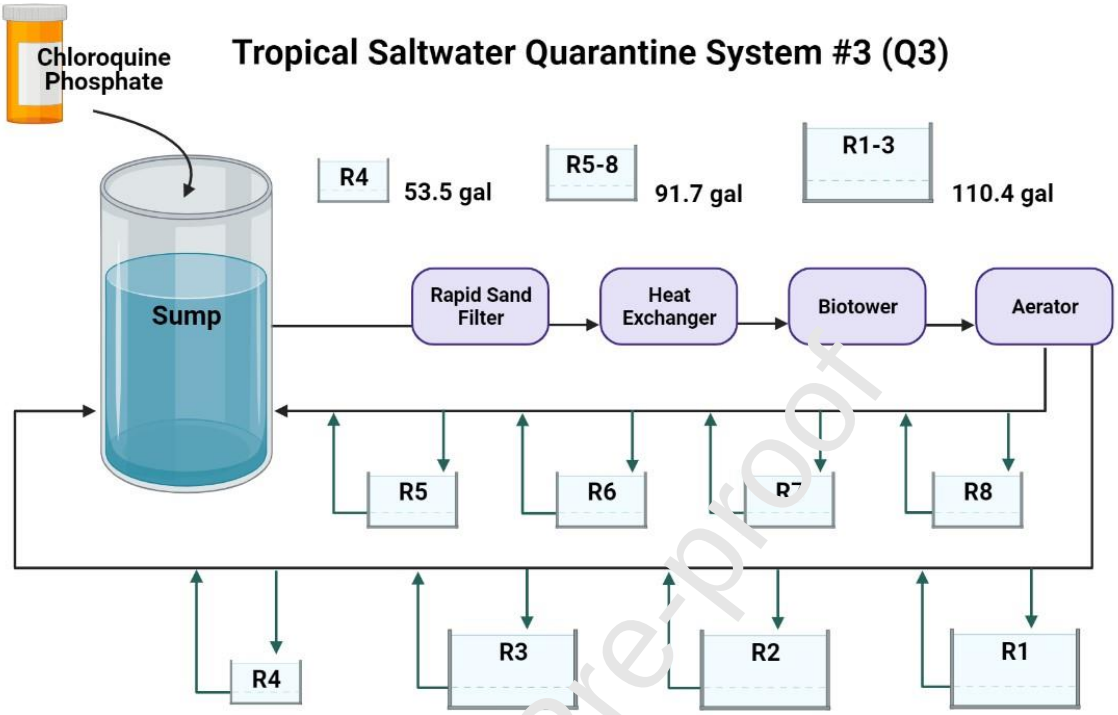

Figure 2

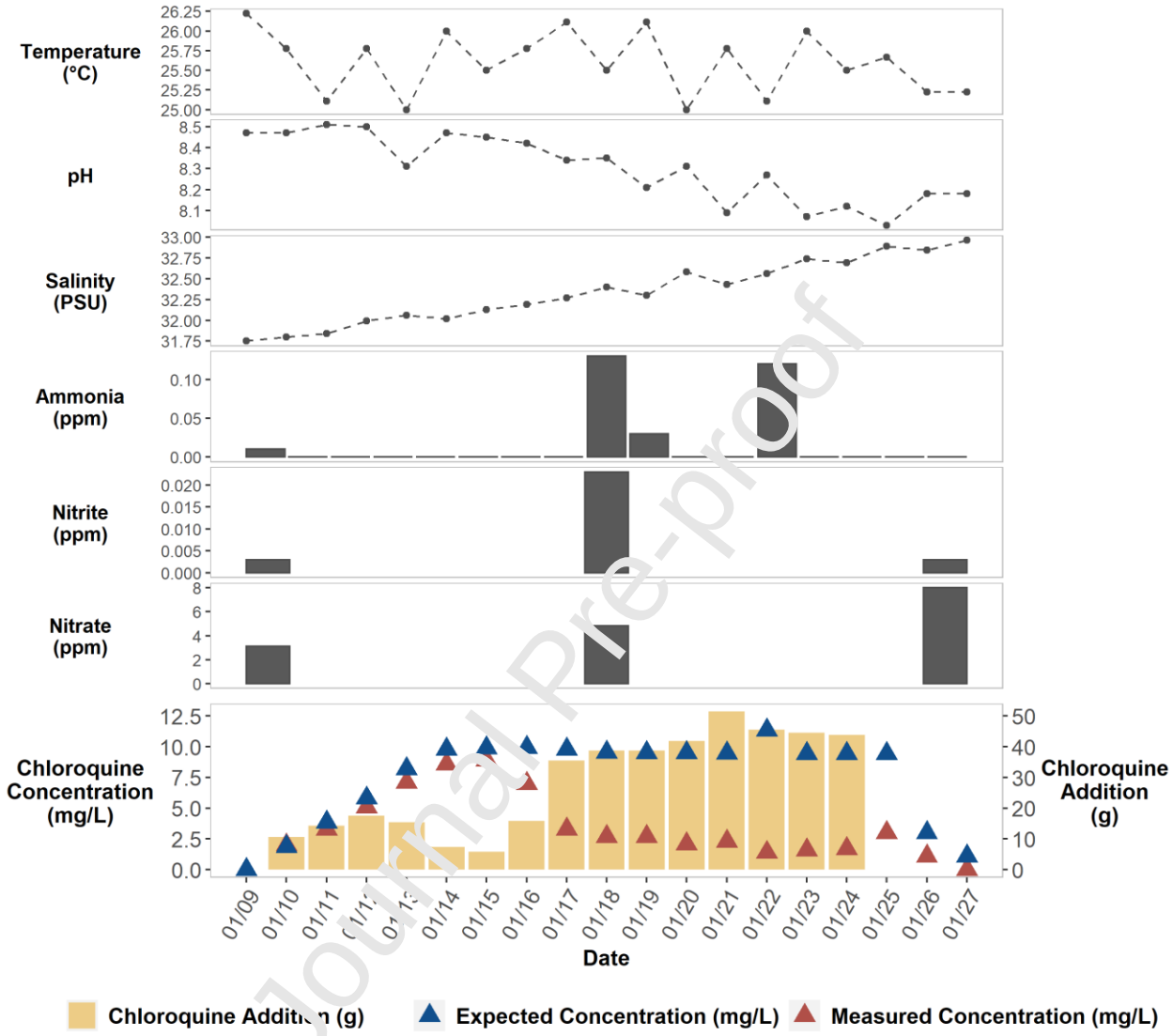

Figure 3

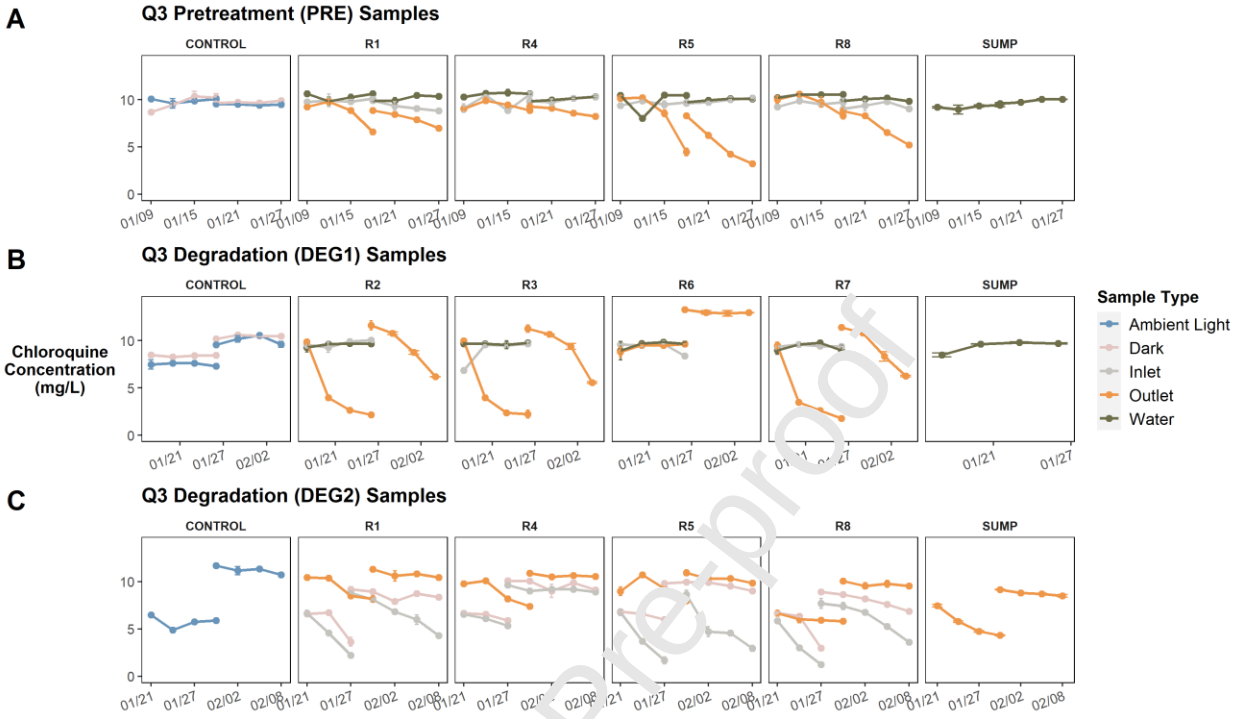

Figure 4

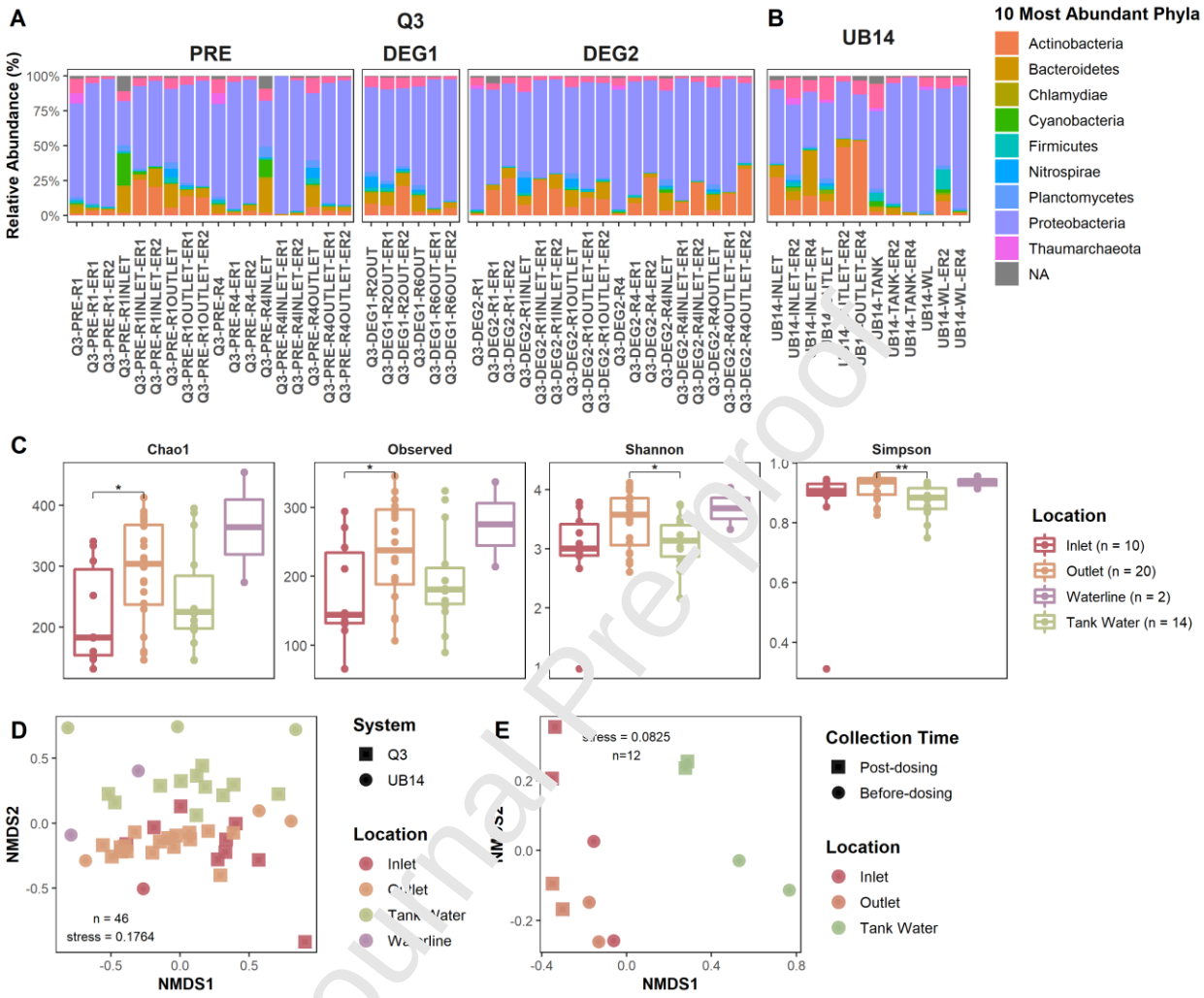

Figure 5

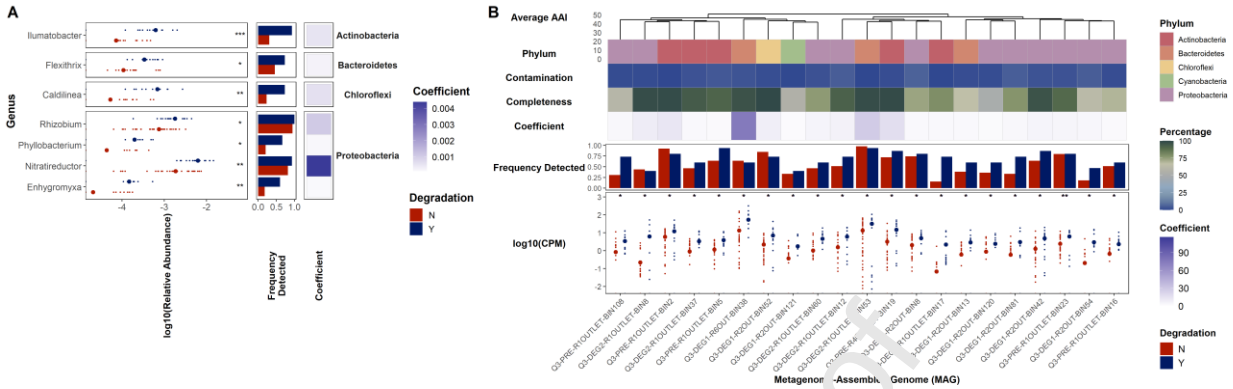

Figure 6

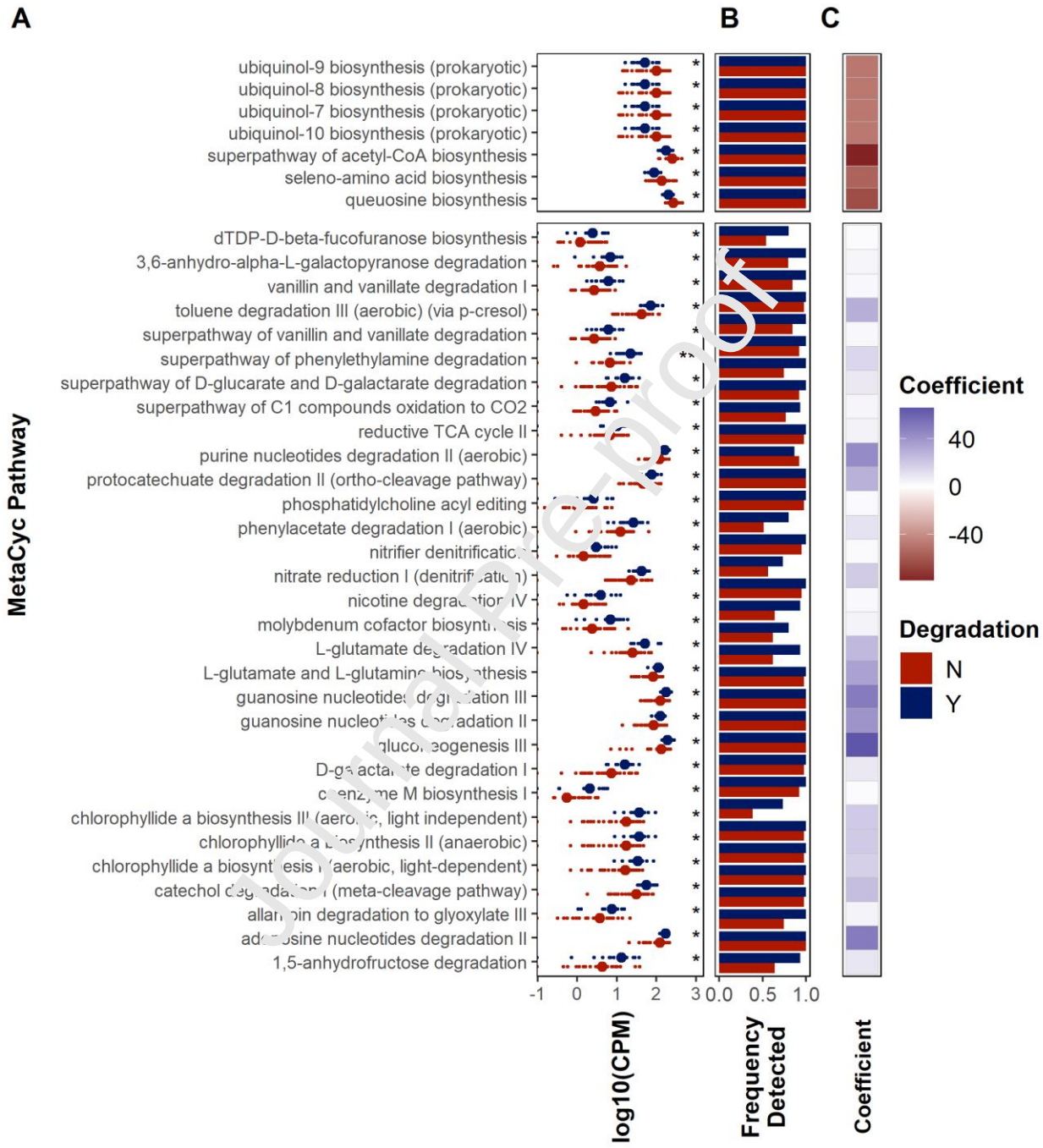

Graphical abstract

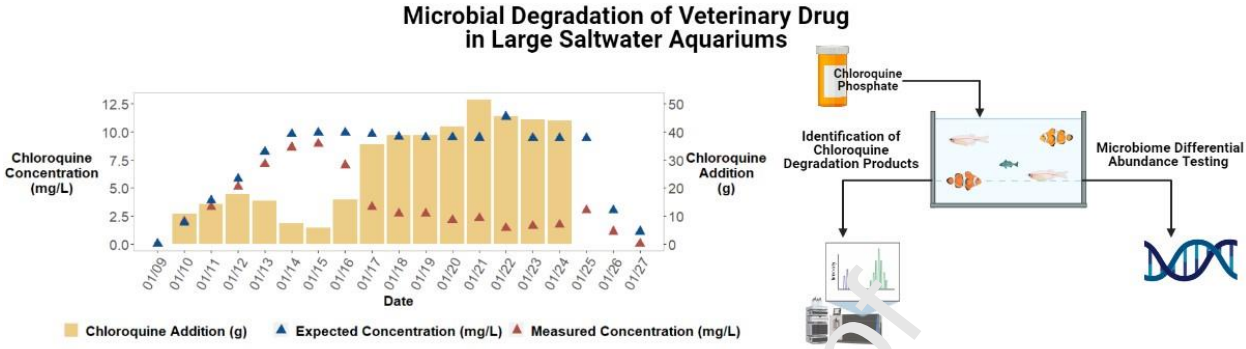

Highlights

- Microbial processes dominate the degradation of chloroquine in saltwater aquariums.
- Pipeline communities represent the main contributors to chloroquine degradation.
- Nitrogen limitation likely affects chloroquine degradation in saltwater aquariums.